JOURNAL OF OPTOELECTRONICS AND ADVANCED MATERIALS Vol. 10, No. 10, October 2008, p. 2694 - 2699

Synthesis of Yttrium Iron Garnet ($Y_3Fe_5O_{12}$) nanopowders by a simple proteic sol-gel process

SARAWUTH LABUAYAI[a,c], SINEENAT SIRI[b,c], SANTI MAENSIRI[a,c,*]
[a] *Small & Strong materials Group (SSMG), Department of Physics, Faculty of Science, Khon Kaen University, Khon Kaen, 40002, Thailand*
[b] *Department of Biochemistry, Faculty of Science, Khon Kaen University, Khon Kaen, 40002, Thailand*
[c] *Integrated Nanotechnology Research Center (INRC), Faculty of Science, Khon Kaen University, Khon Kaen, 40002, Thailand*

Yttrium iron garnet $Y_3Fe_5O_{12}$ nanopowders were synthesized by a proteic sol–gel process using coconut water as a solvent. The polymeric precursors were characterized by TG-DTA to determine the thermal decomposition and crystallization temperature which was found to be at above 800 °C. The $Y_3Fe_5O_{12}$ nanopowders were obtained after calcination of the precursors at various temperatures of 800, 900, 1000, and 1100 °C. The prepared samples were characterized by XRD, SEM, and TEM techniques. The particle sizes estimated from XRD were in the range of 22-55 nm. The size of magnetic nanoparticles increased with increasing calcination temperature. The study of magnetic properties by VSM at room temperature showed that the samples are ferromagnetic, having the specific magnetizations of 2.6, 5.3, 8.3, and 17.1 emu/g at 10 kOe for $Y_3Fe_5O_{12}$ samples calcined at 800, 900, 1000, and 1100 °C, respectively. The cytotoxicity to NIH 3T3 of the prepared $Y_3Fe_5O_{12}$ samples was evaluated by MTT assay. The results showed the low cytotoxicity in the calcined $Y_3Fe_5O_{12}$ samples, which are useful for biomedical applications.

(Received February 13, 2008; accepted August 14, 2008)

Keywords: Yttrium iron garnet, Synthesis, Nanopowders, Magnetic properties, Electron microscopy, Sol-gel process

1. Introduction

The ferromagnetic garnet, yttrium iron garnet ($Y_3Fe_5O_{12}$) and its derived compounds are known as important class of materials due to their magneto-optic properties which lead to several applications including electronic devices such as phase shifters for microwave and circulator and magneto-optical devices [1-3]. Many methods have been used to prepare $Y_3Fe_5O_{12}$ material. The conventional way of producing this material is by solid state reaction of with oxide/carbonate (e.g. Y_2O_3 and Fe_2O_4 powders) and calcined at high temperature (>1200 °C) [4]. However, this method had some inherent disadvantages such as chemical inhomogeneity, coarser particle size, and introduction of impurities during ball milling. To overcome these problems, several techniques have been recently developed for preparations of finer $Y_3Fe_5O_{12}$ powders, including sol-gel auto-combustion process method [5,6], sol-gel method [7,8], coprecipitation method [9] and microemulsion method [10]. The properties of $Y_3Fe_5O_{12}$ particles are strongly affected by the composition and microstructure, which are sensitive to the preparation methodology used in their synthesis. Among other established synthesis methods, simple and cost effective routes to synthesize $Y_3Fe_5O_{12}$ nanopowders by utilization of cheap, nontoxic and environmentally benign precursors are still the key issues.

Recently, a simple solution route using the coconut water (*Cocos nucifera*) as a precursor of organic chain (referred to as a proteic sol–gel) has been successfully used in the preparation of thin films (i.e., $CoFe_2O_4$ [11,12], Y_2O_3 [13], $Li_xMn_2O_4$ [14], and $BaFe_{12}O_{19}$ [15]) and nanopowders (i.e., $NiFe_2O_4$ [16] and $BaFe_{12}O_{19}$ [17]). Since the main composition of coconut water is water, proteins, fats, carbohydrates and mineral salts, the function of the chelating agent in the solution is mainly attributed to the protein, which makes the proteic sol–gel process possible to obtain binary and ternary oxides after heat treatment the precursor at high temperature [18].

In this paper, we demonstrate the applicability of a proteic sol-gel process to the preparation of $Y_3Fe_5O_{12}$ nanopowders with particle size of ~ 22-55 nm using metal nitrates of yttrium (Y) and iron (Fe) as metal source in an aqueous medium of filtered coconut water. The synthesized $Y_3Fe_5O_{12}$ samples were characterized by thermogravimetric-differential thermal analysis (TG-DTA), X-ray diffraction (XRD), scanning electron microscopy (SEM) and transmission electron microscopy (TEM). The magnetic properties of the prepared $Y_3Fe_5O_{12}$ samples were investigated using a vibrating sample magnetometer (VSM) at room temperature. The cytotoxicity to NIH 3T3 of the prepared $Y_3Fe_5O_{12}$ samples was also evaluated by MTT assay.

2. Experimental

$Y(NO_3)_3.6H_2O$ (99.99% Purity, Kento Chemicals, Japan), $Fe(NO_3)_3.9H_2O$ (99.9% Purity, Kento Chemicals, Japan) and filtered coconut water solution were used as the starting materials. In a typical procedure, 7.2843g of $Y(NO_3)_3.6H_2O$ and 12.7121g of $Fe(NO_3)_3.9H_2O$ (a mole ratio corresponding to nominal composition of Y : Fe ratio of 3 : 5) were added slowly to the filtered coconut water solution with vigorous stirring at 37 ºC for 1 h. The initial pH of mixed solution was about 0.81. Then, the mixed solution was evaporated by heating on a hot plate at 100 ºC with vigorous stirring for several hours until a dried precursor was obtained. The dried precursor was crushed into powder using mortar and pestle. In order to determine the temperature of possible decomposition and crystallization of the powders, the dried precursor was subjected to thermogravimetric-differential thermal analysis (TG-DTA) (Pyris Diamond TG-DTA, PerkinElmer Instrument). The crystallization seemed to occur at temperature above 800 ºC (Fig. 1). The dried precursor was then calcined in a box-furnace at 800, 900, 1000 and 1100 ºC for 3 h in air. The final products obtained were dark brown sample.

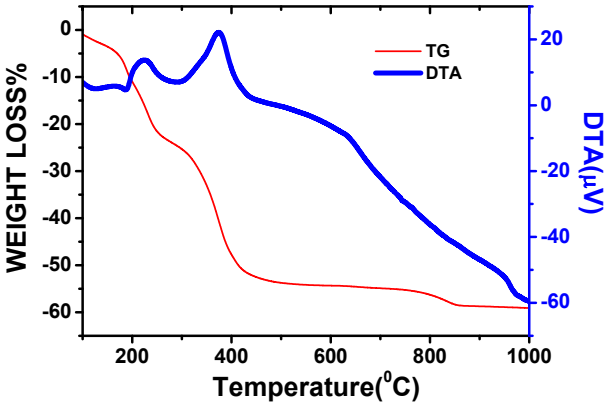

Fig. 1. TG –DTA caves of thermal decomposition of $Y_3Fe_5O_{12}$ precursor at a heating rate of 5 ºC/min in static air.

The prepared samples were characterized for crystal phase identification by powder X-ray Diffraction (XRD) using a Philips X-ray diffractometer (PW3040, The Netherlands) with CuKα radiation (λ = 0.15406 nm). The particle size and external morphology of the fine calcined powders were characterized by scanning electron microscopy (SEM) (LEO 1450VP, U.K.) and transmission electron microscopy (TEM) (JEM 2010, JEOL, Japan). The magnetic properties of the calcined powders were examined at room temperature (20 ºC) using (VSM 7403, Lake Shore, USA).

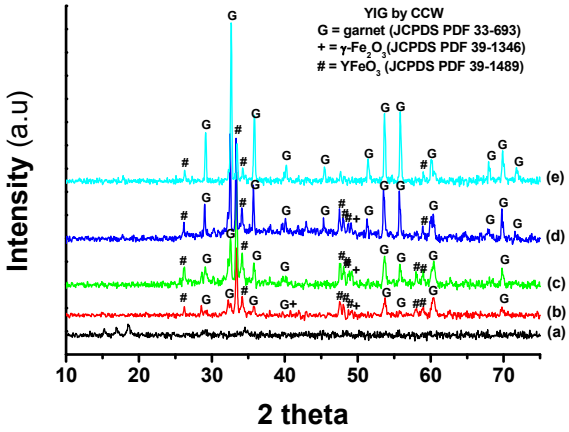

Fig. 2. XRD patterns of (a) precursor and $Y_3Fe_5O_{12}$ samples calcined in air at (b) 800, (c) 900, (d) 1000 and (e) 1100 ºC for 3 h.

For cell culture and maintenance, Mouse fibroblasts (NIH 3T3) were cultured in Dulbecco's modified Eagle's medium (DMEM; Sigma-Aldrich, USA) supplemented with 10% fetal bovine serum (FBS; Gibco BRL, USA) and 100U penicillin/ 1 mg/ml streptomycin (Sigma-Aldrich, USA). Medium was replaced once in every 2 days and the cell cultures were maintained in an incubator at 37°C and 5% CO_2 humidified atmosphere. The cytotoxicity of the samples were evaluated with NIH 3T3 and viable cells were measured by MTT colorimetric assay (Sigma, USA). Cells at 80-90% confluence were trypsinized and 1 x 10^4 cells were seeded on each well of 96-well culture plate for 24 h. The extracted $Y_3Fe_5O_{12}$ liquid was performed in sterile distilled water at 121°C for 1 h with the ratio of 0.2 g/ml. Cells were incubated with 20 µl extracted $Y_3Fe_5O_{12}$ liquid and sterile water (control) for 24 h. After removal of the medium, 10 µl of 12 mM MTT solution was added and the cells were incubated for further 4h. Blue formazan crystals, metabolized MTT in mitochondria of viable cells, were dissolved in 50 µl of dimethylsulfoxide (DMSO; Sigma, USA) and measured at 550 nm by the plate reader (Biorad, Japan). The average value of 4 wells was used for each sample and two repeats were done in each experiment. The control NIH 3T3 cell viability was defined as 100%. Statistical comparison was performed using one-way ANOVA with SPSS software version 11.5 (SPSS, Germany). P value < 0.05 was considered statistically significant.

3. Results and discussion

The TG curve in Figure 1 shows a minor weight loss step from 100 ºC up to about 280 ºC and major weight loss step from ~280 ºC up to about 400 ºC. The minor weight loss was related to the losses of moisture and trapped solvent (water and carbon dioxide), while the major weight loss was due to the combustion of organic matrix.

On the DTA curve, two main exothermic peaks were observed at ~221 and 372 ºC, suggesting that the thermal events related to the burn-out of organic species in the precursor. The plateau formed between 850-1000 ºC on the TG curve indicated the formation of $Y_3Fe_5O_{12}$ as the decomposition product, as confirmed by XRD analysis, shown in Fig. 2.

XRD patterns of all samples in Fig. 2 show typical peak patterns, which can be indexed as the $Y_3Fe_5O_{12}$ structure in the standard data (JCPDS, 33-363) [6,19,20]. However, the presence of second phases such as γ- Fe_2O (JCPDS, 39-1346) and $YFeO_3$ (JCPDS, 39-1489) are also detected [20,21]. The values of lattice parameter (a) determined from XRD results are 1.20386, 120271, 1.19328 and 1.19684 nm for the powder samples calcined at 800, 900, 1000 and 1100 ºC, respectively. These values close to that of lattice constant a = 1.2377 nm in the standard data (JCPDS, 33-363). The crystallite sizes of the powders were estimated from X-ray line broadening using Scherrer's equation [22] (i.e. $D = 0.89k/ (\beta\cos\theta)$, where k is the wave-length of the X-ray radiation, K is a constant taken as 0.89, θ is the diffraction angle. β is the full width at half maximum (FWHM)), and were obtained to be 22, 30, 33 and 55 nm for the powder calcined at 800, 900, 1000 and 1100 ºC, respectively.

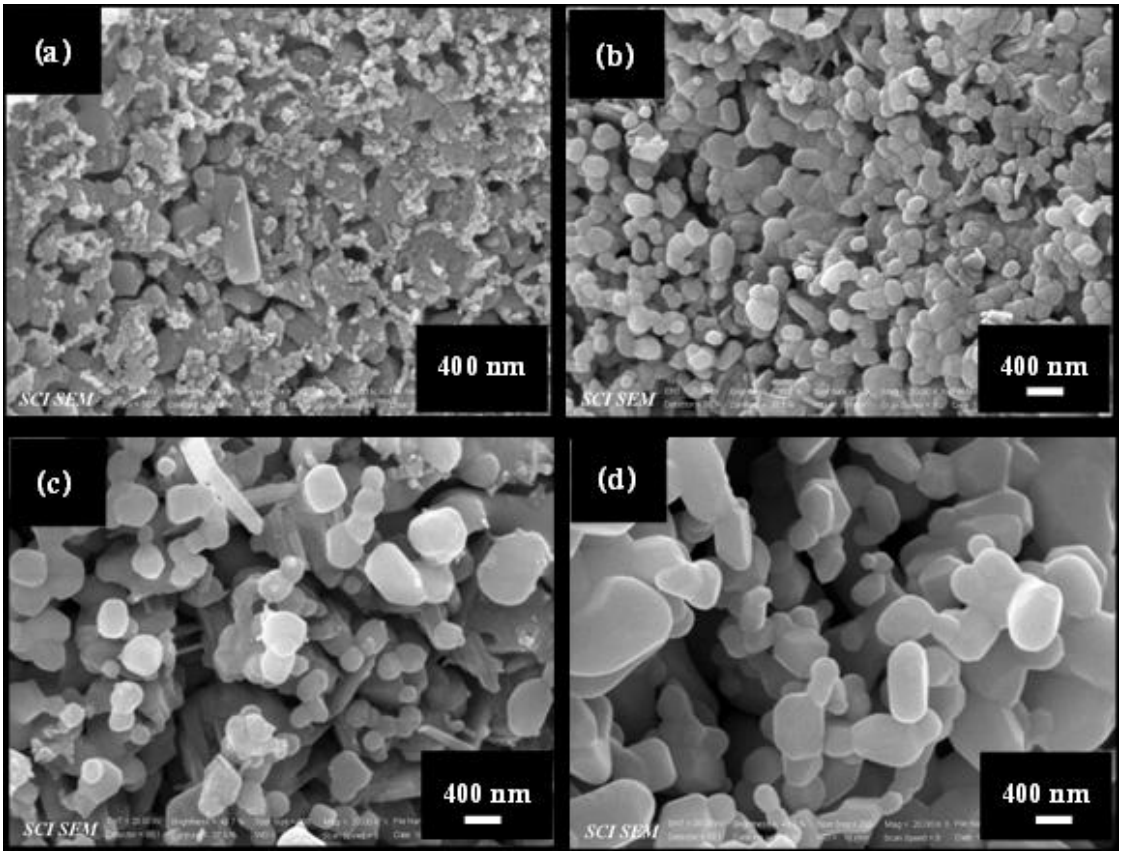

Fig. 3. SEM micrographs of $Y_3Fe_5O_{12}$ samples calcined in air at (b) 800, (c) 900, (d) 1000 and (e) 1100 ºC for 3 h.

Morphology of the calcined $Y_3Fe_5O_{12}$ powders was revealed by SEM as shown in Figure 3. The powder sample calcined at 800 ºC consists of small particles (<50 nm) and large agglomerate particles (~200 nm-2 μm), while the powder sample calcined at 900 ºC contains agglomerate particles having size in the range of 50-400 nm. The 1000 ºC-calcined sample and 1100 ºC-calcined sample also contain agglomerate particles having size in the ranges of 200-600 nm, and 400-1000 nm, respectively. It is noted that the particles size estimated by SEM are larger than those obtained from X-ray line broadening. This is due to agglomeration of the nanoparticles in the powder samples. It is clearly seen from the SEM results that the particle size of the powder increased with increasing calcination temperature.

The morphology of the samples was further investigated by TEM. Fig. 4 shows TEM bright-field images of the calcined $Y_3Fe_5O_{12}$ samples. It is obvious that the morphology and size of the samples was affected by the calcination temperatures. The $Y_3Fe_5O_{12}$ sample calcined at 800 ºC contains agglomerate nanoparticles with diameter ~ 20-100 nm. The differences in morphology and size of these particles can be an indication of their difference phase structures and composition. The 900 ºC and 1000 ºC calcined samples consist of linked particles of ~100-200 nm in diameter. The $Y_3Fe_5O_{12}$ sample calcined at 1100 ºC contains a large particle with particle size of ~ 250-300 nm.

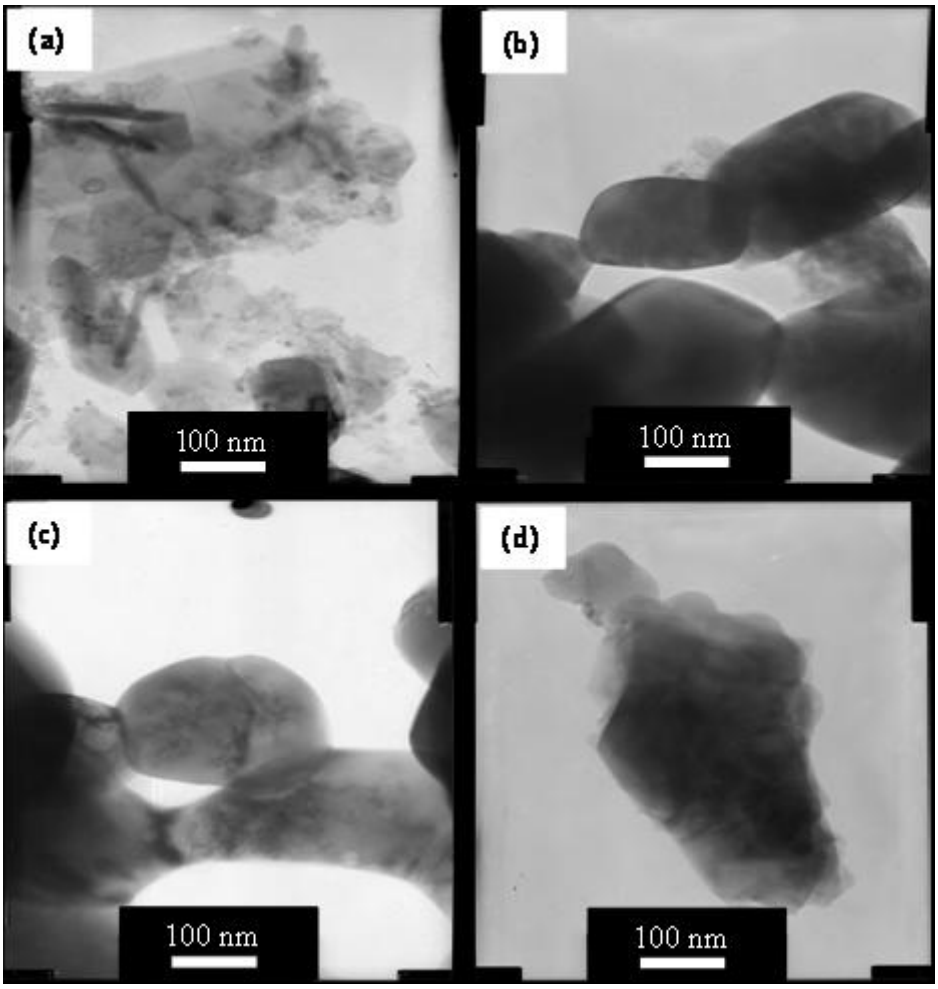

Fig. 4. TEM images of $Y_3Fe_5O_{12}$ samples calcined in air at (a) 800, (b) 900, (c) 1000 and (d) 1100 ºC for 3 h.

The specific magnetization curves of calcined $Y_3Fe_5O_{12}$ sample obtained from room temperature (20 °C) are presented in Fig. 5. These curves are typical for a soft magnetic material. They indicate hysteresis ferromagnetism in the field range of ±500 Oe, while out side this range the specific magnetization increases with increasing field and saturates in the field range investigated ±10 kOe. Specific saturation magnetization (M_s) values of 2.6, 5.3, 8.3 and 17.1 emu/g were observed for $Y_3Fe_5O_{12}$ samples calcined at 800, 900, 1000 and 1100 ºC, respectively. These values are comparable to those of 6-21 emu/g for the $Y_3Fe_5O_{12}$ nanoparticles of 9-25 nm reported by Rajendran et al. [19]. It is found that the tendency of M_s increase is consistent with the enhancement of crystallinity, and the values of M_s for the $Y_3Fe_5O_{12}$ samples were observed to increase with increasing particle size as reported previously by other research groups [7, 19, 23]. Figure 6 shows the values of magnetization and coercivity as a function of calcination temperature for the synthesized $Y_3Fe_5O_{12}$ samples. The coercivity (H_c) of $Y_3Fe_5O_{12}$ samples decreases with increasing calcination temperature. It is seen that the coercivity is lager and the magnetization is smaller for the sample having smaller particle size, indicating the larger anisotropy of the particles with smaller size [19].

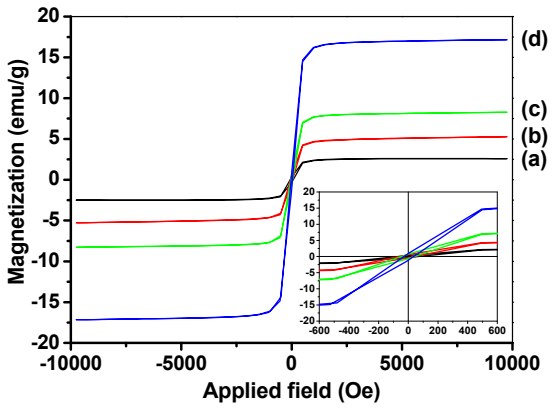

Fig. 5. The specific magnetization of $Y_3Fe_5O_{12}$ samples as a function of field, measured at 20°C. The samples were calcined in air at (a) 800, (b) 900, (c) 1000 and (d) 1100 °C for 3 h. The inset shows the low-field region of ± 600 Oe.

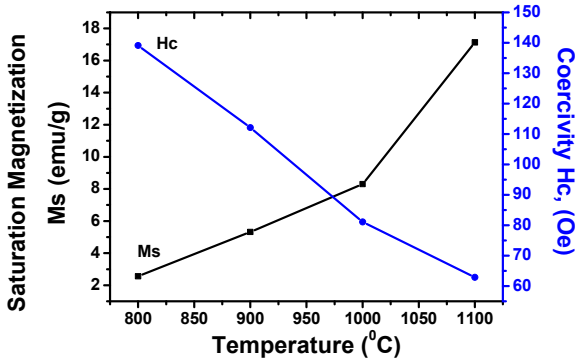

Fig. 6. Magnetizetion and coercivity of $Y_3Fe_5O_{12}$ samples as a function of calcination temperature.

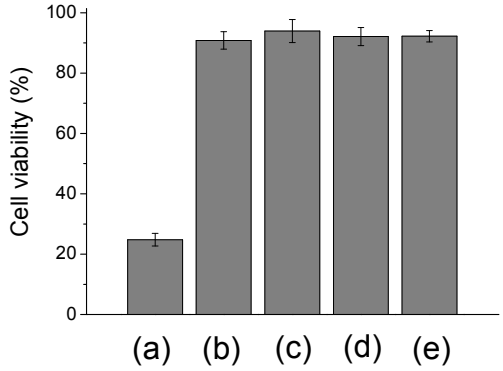

Fig. 7. NIH 3T3 Cell Viability in response to the extraction liquid of $Y_3Fe_5O_{12}$ precursor and $Y_3Fe_5O_{12}$ powders calcined in air at (a) 800, (b) 900, (c) 1000, and (d) 1100 ℃, for 3 h. Cell viability was measured after the incubation at 37℃ for 24 h. (n=4, $p < 0.05$)

The cytotoxicity of $Y_3Fe_5O_{12}$ samples was evaluated by measuring viable cells after 24 h of incubation with the magnetic extracted liquids, and the results are shown in Fig. 7. The results showed that precursor $Y_3Fe_5O_{12}$ sample was highly toxic to the cells as seen from the results of cell viability at 24.8% (Fig. 7). However, the cytotoxicity of the $Y_3Fe_5O_{12}$ samples calcined in air at 800, 900, 1000, and 1100 °C for 3 h, was greatly reduced. The cytotoxicity of the $Y_3Fe_5O_{12}$ samples calcined at 800, 900, 1000, and 1100 °C was less than 20% in all samples (Fig. 7). The cell viability results were 90.8 ± 2.9, 93.9 ± 3.8, 92.1 ± 3.0, and 92.2 ± 1.9%, respectively. The low cytotoxicity of the calcined $Y_3Fe_5O_{12}$ samples suggests their potential applications in biomedicine.

4. Conclusions

We have successfully synthesized $Y_3Fe_5O_{12}$ nanopowders by a proteic sol–gel process using coconut water as a solvent. In this proteic sol–gel process, the proteins form the chain where yttrium and iron ion(s) were bound and formed an organic precursor upon heating at low temperature. After having been calcined at 800, 900, 1000, and 1100 °C, the precursor was transformed into $Y_3Fe_5O_{12}$ nanopowders. The prepared samples were characterized by XRD, SEM, and TEM techniques. The size of magnetic nanoparticles increased with increasing calcination temperature. The calcined $Y_3Fe_5O_{12}$ nanopowder samples are ferromagnetic, having the specific magnetizations of 2.6-17.1 emu/g at 10 kOe. The magnetization of samples increased with increasing particle size, while the coercivity decreased with increasing particle size which is due to the larger anisotropy of the particles with smaller size. The $Y_3Fe_5O_{12}$ precursor was highly toxic to the NIH 3T3 cells, whereas the calcined samples showed a reduction in their toxicity to the cells.

Acknowledgements

The authors would like to thank the Department of Chemistry, Khon Kaen University for providing TG-DTA and VSM facilities, and the Department of Physics, Ubon Ratchathanu University for providing XRD facilities, and the Science and Technology Service Center (Chiang Mai University) for providing TEM facilities. This work is partially supported by The National Nanotechnology Center (NANOTEC), NSTDA, Ministry of Science and Technology, Thailand, through its program of Center of Excellent.

References

[1] T. Y. Kim, Y. Yamazaki, T. Hirano, Phys. Status Solidi B **241**(7), 1601 (2004).
[2] Y. H. Jeon, J. W. Lee, J. H. Oh, J. C. Lee, S. C. Choi, Phys. Status Solidi A **201**(8), 1893 (2004)
[3] S. Taketomi, C. M. Sorensen, K. J. Klabunde, J. Magn. Magn. Mater. **222,** 54 (2000).
[4] H. Zhao, J. Zhou, Y. Bai, Z. Gui, L. Li, J. Magn. Magn. Mater. **280,** 208 (2004).
[5] S. Hosseini Vajargah, H. R. Madaah Hosseini, Z. A. Nemati, Mater. Sci. Eng. B **129,** 211 (2006).
[6] S. Hosseini Vajargah, H. R. Madaah Hosseini, Z. A. Nemati, J. Alloy. Compd. **430**, 339 (2007).
[7] Z. Cheng, Hua Yang, J. Physica E. **39**, 198 (2007).
[8] R. D. Sanchez, J. Rivas, P. Vaqueiro, M. A. Lopez-Quintela, D. Caeiro, J. Magn. Magn. Mater. **247**, 92 (2002).
[9] M. Jafelicci Jr., R.H.M. Godoi, J. Magn. Magn. Mater. **226-230,** 1421 (2001).
[10] A. G. Teijerio, D. Baldomir, J. Ravas, S. Paz, P. Vaqueiro, A. Lopez Quintela, J. Magn. Magn. Mater. **140-144,** 2129 (1995).
[11] J. G. S. Duque, M. A. Macedo, N. O. Moreno, Phys. Status Solidi (b) **220**, 413 (2000).
[12] J. G. S. Duque, M. A. Macedo, N. O. Moreno, J. L. Lopez, H. D. Pfanes, J. Magn. Magn. Mater.

226–230, 1424 (2001).
[13] P. J. R. Montes, M. E. G. Valerio, M. A. Macedo, F. Cunha, J. M. Sasaki, Microelectron. J. **34**, 557 (2003).
[14] C. T. Meneses, M. A. Macedo, F. C. Vicentin, Microelectron. J. **34**, 561 (2003) .
[15] J. V. A. Santos, M. A. Macedo, F. Cunha, J. M. Sasaki, J. G. S. Duque, Microelectron. J. **34**, 565 (2003).
[16] M.N.B. Silva, J.G.S. Duque, D.X. Gouveia, J.A.C. de Paiva, M.A. Macedo, Jpn. J. Appl. Phys. **43**, 5249 (2004).
[17] P. C. A. Brito, R. F. Gomes, J. G. S. Duque, M A. Macedo, J. Physica B. **384**, 91 (2006).
[18] M.A. Macedo, M.N.B. Silva, A.R. Cestari, E.F.S. Vieira, J.M. Sasaki, J.C. Goes, J.A. Aguiar, Physica B: Condens. Matter **354**, 171 (2004).
[19] M. Rajendran, S. Deka, P.A. Joy, A.K. Bhattcharya, J. Magn. Magn. Mater. **301,** 212 (2006).
[20] P.Vaqueiro, M. P. Crosnier-Lopez, and M. A. Lopez-Quintela, J. Solid. Stete. Chem. **161,** 161 (1996).
[21] X.Z. Guo, B.G Ravi, P.S. Devi, J.C. Hanson, Magolies, R.J. Gambino, J.B. Paris, S. Sampath, J. Magn. Magn. Mater. **295**, 145 (2005).
[22] B. D. Cullity, S.R. Stock, Elements of X-ray Diffraction, 3ed., Prentice Hall, New Jersey, 2001.
[23] Z. Cheng, H. Yang, L. Yu, Y. Cui, S. Feng, J. Magn. Magn. Mater. **302**, 259 (2006).

*Corresponding author: sanmae@kku.ac.th;
santimaensiri@gmail.com